



Simulation of biodegradation process in a fluidized bed bioreactor using genetic algorithm trained feedforward neural network

A. Venu Vinod*, K. Arun Kumar, G. Venkat Reddy

Department of Chemical Engineering, National Institute of Technology, Warangal 506 004, India

ARTICLE INFO

Article history:

Received 1 November 2008

Received in revised form 27 March 2009

Accepted 14 April 2009

Keywords:

Biofilm
Immobilized
Waste treatment
Biodegradation
Neural network
Genetic algorithm

ABSTRACT

The biodegradation process of phenol in a fluidized bed bioreactor (FBR) has been simulated using genetic algorithm trained feedforward neural network. Experiments were carried out using the microorganism *Pseudomonas* sp. on synthetic wastewater. The steady state model equations describing the biodegradation process have been solved using feedforward artificial neural network (FFANN) and genetic algorithm (GA). The mathematical model has been directly mapped onto the network architecture and the network has been used to find an error function (mean squared error criterion). The minimization of the error function with respect to network parameters (weights and biases) has been considered as training of the network. Real-coded genetic algorithm has been used for training the network in an unsupervised manner. The diffusivities of phenol and oxygen in biofilm obtained from the simulation have been compared with the literature values.

© 2009 Elsevier B.V. All rights reserved.

1. Introduction

Fluidized bed bioreactors have been receiving considerable interest in wastewater treatment. The fluidized bed bioreactor has been shown [1–5] to outperform other types of reactors. The superior performance of the fluidized bed bioreactor is due to very high biomass concentration due to immobilization of cells onto the solid particles; intimate contact between gas, liquid and solid phases; decoupling of residence times of liquid and microbial cells due to immobilization. Extensive information is available in literature on the biodegradation of phenol and fluidized bed bioreactors [6–14]. Phenolic wastewater treatment is done by using methods like freely suspended cell systems, trickling filters, rotating disc, activated sludge, biological fixed film methods and fluidized bed bioreactors. Trickling filters are more advantageous over freely suspended cell systems [1]. However fluidized bed bioreactors have been found to be superior to other type of reactors [4,5] in relation to volumetric biodegradation capacity. A number of attempts have been made to develop mathematical model for biodegradation of phenolic compounds in wastewater [2,3,12]. The present work reports studies with high phenol concentration in feed at 1254 ppm. Mathematical model describing the biodegradation process consists of coupled second order nonlinear ordinary differential equations. These equations are not amenable to analyt-

ical solution, and numerical solution (using, e.g., finite difference, orthogonal collocation, Galerkin finite element) is required.

In early-1990s it was proved that the approximation capabilities of networks make ANN as numerically accurate and predictable as conventional computational methods [15–17]. Neural networks can be more advantageous than the conventional techniques. Finding a neural network that approximates the solution of a given set of differential equations has many benefits compared with traditional numerical methods viz., obtaining an analytic continuous solution (compared to numerical methods), good generalization capabilities, tackling real time problems reaching the global minimum of the error surface, etc. [15,17,18].

The model equations for biodegradation of phenol have been previously simulated using conventional numerical methods [2,3,12]. These studies involved lower concentrations of phenol: 38–72 mg/l [2,3] and 82–131 mg/l [12]. In view of the advantages cited above, in this work an attempt has been made to solve the steady state model equations describing the biodegradation process of phenol using a combination of neural network–GA. Previous studies [3,12] involved prediction of the values of diffusivities of phenol and oxygen in biofilm at low concentrations of phenol mentioned above. In this study the diffusivities have been obtained at high concentration of phenol (1254 mg/l).

2. Mathematical modeling

A model describing the biodegradation of phenol by bacteria immobilized onto the plastic beads was used which is similar to

* Corresponding author. Tel.: +91 870 2462621; fax: +91 870 2459547.
E-mail address: avv122@yahoo.com (A. Venu Vinod).

Nomenclature

B	differential operator
Bi_i	dimensionless group ($k_o\delta/D_{of}$)
Bi_s	dimensionless group ($k_s\delta/D_{sf}$)
C	dissolved oxygen concentration in biofilm (kg/m^3)
C_b	dissolved oxygen concentration in the bulk liquid phase (kg/m^3)
C_i	dissolved oxygen concentration at the interface between a bioparticle and the bulk liquid (kg/m^3)
C^*	dimensionless dissolved oxygen concentration (c/c_b)
D	differential operator
D_{of}	diffusion coefficient of oxygen in biofilm (m^2/s)
D_{ow}	diffusion coefficient of oxygen in water (m^2/s)
D_{sf}	diffusion coefficient of phenol in biofilm (m^2/s)
D_{sw}	diffusion coefficient of phenol in water (m^2/s)
E	error measure
$f^*(y)$	approximated output from the network
k_o	liquid–solid mass transfer coefficient for oxygen (m/s)
k_s	liquid–solid mass transfer coefficient for phenol (m/s)
K_i	inhibition constant for phenol (kg/m^3)
K_o	Monod constant for oxygen (kg/m^3)
K_s	Monod constant for phenol (kg/m^3)
K_i^*	dimensionless inhibition constant for phenol
K_o^*	dimensionless Monod constant for oxygen
K_s^*	dimensionless Monod constant for phenol
N_p	number of bioparticles in FBR
N	output of the network
n	number of inputs to the FFANN
$nPOP$	population size
p_c	crossover probability
P	number of points in the integration domain
P_B	total number of boundary points
Q	flow rate of synthetic wastewater (m^3/s)
r	radial coordinate in biofilm (m)
r_p	radius of biomass-free bioparticle (m)
R_{obs}	observed rate of phenol removal in the reactor (kg/s)
R_{scal}	calculated rate of phenol removal in the reactor (kg/s)
S	phenol concentration in biofilm (kg/m^3)
S_b	phenol concentration in the bulk liquid (kg/m^3)
S_i	phenol concentration in inlet synthetic wastewater (kg/m^3)
S_i	phenol concentration at the interface between a bioparticle and the bulk liquid (kg/m^3)
S^*	dimensionless phenol concentration (S/S_b)
t	time (s)
u_i, u_{out}	bias of hidden unit i and output unit, respectively
v_i	weight from the hidden unit i to the output unit
w_{ij}	weight from the input unit j to the hidden unit i
x	dimensionless distance ($(r - r_p)/\delta$)
\vec{x}	input vector
$Y_{x/s}$	yield coefficient ($\text{kg biomass}/\text{kg phenol}$)
$Y_{x/o}$	yield coefficient ($\text{kg biomass}/\text{kg oxygen}$)
Greek letters	
δ	biofilm thickness (m)
ρ_v	biofilm density (kg/m^3)
μ	specific growth rate of biomass ($\text{s}^{-1}, \text{h}^{-1}$)
μ_{max}	maximum specific growth rate of biomass ($\text{s}^{-1}, \text{h}^{-1}$)
ϕ_o	dimensionless modulus for oxygen

ϕ_s	dimensionless modulus for phenol
φ	sigmoid transfer function
φ', φ''	first and second derivatives of sigmoid transfer function, respectively

the one employed by Tang and Fan [3]. Phenol and oxygen were assumed to be simultaneously diffusing into and reacting within the film. There are three basic processes occurring in the biodegradation of phenol in a fluidized bed bioreactor:

- Transport of oxygen from the gas phase into the bulk liquid.
- Transport of phenol, oxygen and other nutrients from the bulk liquid phase to the surface of the film.
- Simultaneous diffusion and reaction of phenol, oxygen and other nutrients within the biofilm.

Process (a) was not considered in this work, as dissolved oxygen concentration was maintained constant.

Steady state is reached in the completely mixed draft-tube, three phase fluidized bed bioreactor when the bulk concentrations of phenol and oxygen are constant and the change in biofilm properties such as the film thickness and density are negligible. Therefore the concentration profiles of phenol and oxygen in the biofilm are independent of time. The following assumptions were made in the development of the model:

- The FBR is in backmix condition,
- Biomass loading is constant at steady state,
- Plastic bead particles are spherical and inert,
- Biomass coating on particles is uniform,
- The growth limiting nutrients are phenol and oxygen. All other nutrients are in excess. The growth kinetics are assumed to follow Monod kinetics with respect to oxygen and substrate inhibited kinetics with respect to phenol.

$$\mu = \frac{\mu_{max}S}{(S+K_S+S^2/K_i)} \frac{C}{(K_o+C)} \quad (1)$$

- The biofilm has same kind of effect on phenol and oxygen diffusivities, i.e., the ratio of D_{of}/D_{ow} is the same as the ratio D_{sf}/D_{so} . The diffusivities of the oxygen and phenol are reduced to the same extent in the biofilm compared to that in water.
- Immobilization of cells onto the biofilm does not change the kinetic parameters describing the growth.

With these assumptions mass balances of phenol and oxygen across the biofilm have been carried out to get the following two differential equations:

For phenol:

$$\frac{D_{sf}}{r^2} \left[\frac{d}{dr} \left(r^2 \frac{dS}{dr} \right) \right] - \frac{\rho_v}{Y_{x/o}} \frac{\mu_{max}S}{(S+K_S+S^2/K_i)} \frac{C}{(K_o+C)} = 0 \quad (2)$$

For oxygen:

$$\frac{D_{of}}{r^2} \left[\frac{d}{dr} \left(r^2 \frac{dC}{dr} \right) \right] - \frac{\rho_v}{Y_{x/o}} \frac{\mu_{max}S}{(S+K_S+S^2/K_i)} \frac{C}{(K_o+C)} = 0 \quad (3)$$

The boundary conditions for these equations are

$$\left(\frac{dS}{dr} \right) = \left(\frac{dC}{dr} \right) = 0 \quad \text{at } r = r_p \quad (4)$$

$$D_{sf} \left(\frac{dS}{dr} \right) = k_s(S_b - S_i) \quad \text{at } r = r_p + \delta \quad (5)$$

$$D_{of} \left(\frac{dC}{dr} \right) = k_o(C_b - C_i) \quad \text{at } r = r_p + \delta \quad (6)$$

After solving Eqs. (2)–(6) the rate of phenol degradation from the model can be calculated using the formula:

$$R_{s\text{cal}} = \frac{N_p \rho_v}{Y_{x/s}} \int_{r=r_p}^{r=r_p+\delta} \frac{\mu_{\max} S}{(S + K_S + S^2/K_i)} \frac{C}{(C + K_0)} 4\pi r^2 dr \quad (7)$$

The above rate of biodegradation can be compared with the experimental rate of biodegradation calculated using the formula:

$$R_{S\text{obs}} = Q(S_I - S_b) \quad (8)$$

Eqs. (2)–(6) can be rewritten in terms of dimensionless variables as follows:

$$\frac{d^2 S^*}{dx^2} + \frac{2}{(x + r_p/\delta)} \frac{dS^*}{dx} = \phi_s \frac{S^*}{(S^* + K_s^* + S^{*2}/K_i^*)} \frac{C^*}{(C^* + K_0^*)} \quad (9)$$

$$\frac{d^2 C^*}{dx^2} + \frac{2}{(x + r_p/\delta)} \frac{dC^*}{dx} = \phi_o \frac{S^*}{(S^* + K_s^* + S^{*2}/K_i^*)} \frac{C^*}{(C^* + K_0^*)} \quad (10)$$

$$\left(\frac{dS^*}{dx}\right) = \left(\frac{dC^*}{dx}\right) = 0 \quad \text{at } x = 0.0 \quad (11)$$

$$\frac{dS^*}{dx} = Bi_s(1 - S^*) \quad \text{at } x = 1.0 \quad (12)$$

$$\frac{dC^*}{dx} = Bi_o(1 - C^*) \quad \text{at } x = 1.0 \quad (13)$$

where

$$S^* = \frac{S}{S_b}, \quad C^* = \frac{C}{C_b}, \quad x = \frac{r - r_p}{\delta}, \quad K_s^* = \frac{K_s}{S_b}, \quad K_i^* = \frac{S_b}{K_i}, \quad K_0^* = \frac{K_0}{C_b},$$

$$\phi_o = \frac{\rho_v \mu_{\max} \delta^2}{Y_{x/o} D_{of} C_b}, \quad \phi_s = \frac{\rho_v \mu_{\max} \delta^2}{Y_{x/s} D_{sf} S_b}, \quad Bi_s = \frac{k_s \delta}{D_{sf}}, \quad Bi_o = \frac{k_o \delta}{D_{of}}$$

3. Experimental

3.1. The reactor set-up

The schematic diagram of the draft-tube fluidized bed bioreactor used in the present work is shown in Fig. 1.

3.2. Reactor and the draft-tube

The fluidized bed bioreactor and the draft-tube are made up of glass. A sparger made up of same material has been provided at the bottom of the reactor through which air can be sparged into the reactor. The total volume of the reactor is about $2.67 \times 10^{-3} \text{ m}^3$ (2.67 l). The top of the glass reactor is closed with a plate through which all the probes and sensors are inserted into the reactor. An overflow line has been provided near the top so that, the reaction medium flows out of the reactor in continuous operation.

Plastic beads with a density of 1005 kg/m^3 have been used for immobilization of the microorganism. The average diameter of the beads is 4.31 mm. Two peristaltic pumps one each for media and feed into the reactor have been provided. The flow rate of these pumps can be set at the required value using a flow controller. The capacity of the pumps is 0.11×10^{-7} to $9.7 \times 10^{-7} \text{ m}^3/\text{s}$ (40–3500 ml/h). The reactor is provided with a glass jacket to maintain the temperature of the reactor system. Separate tanks made of

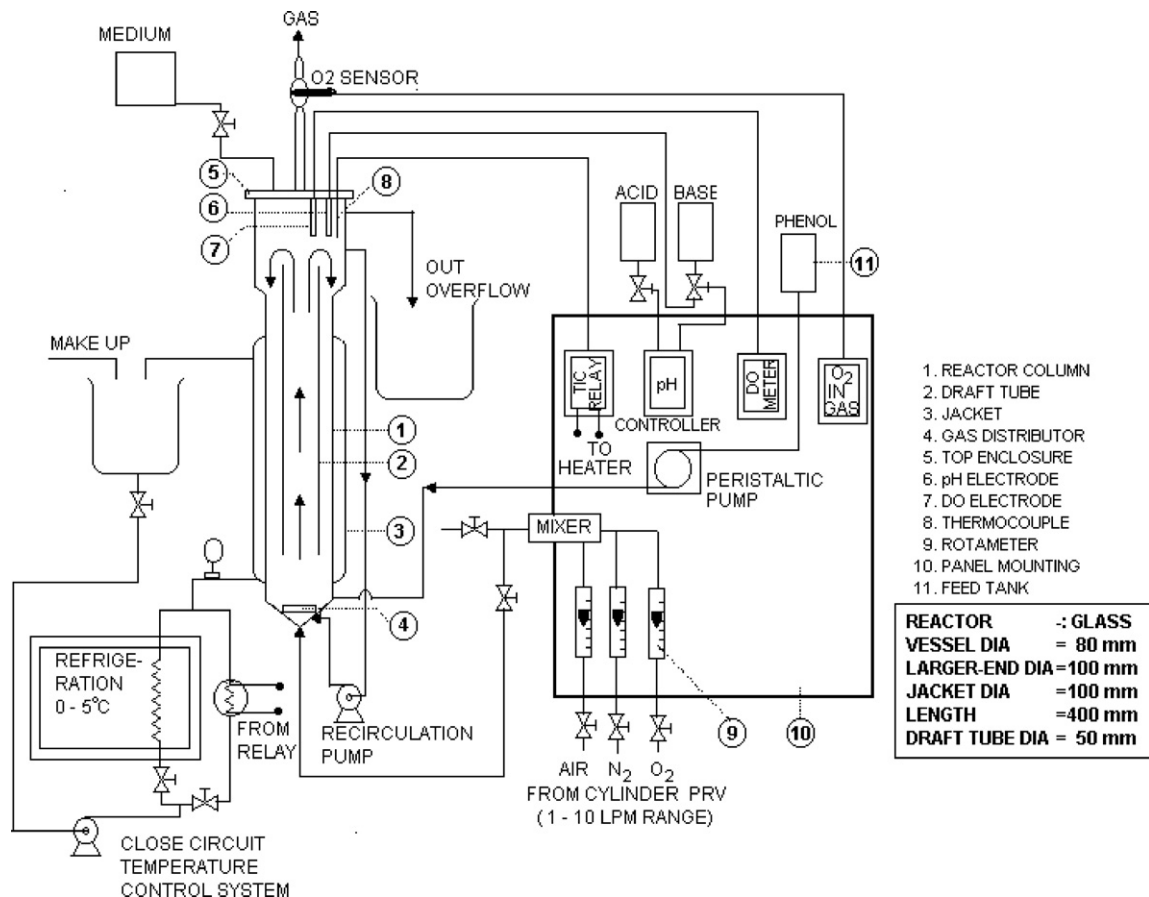


Fig. 1. The experimental set-up for the biodegradation of phenol in a fluidized bed bioreactor.

stainless steel have been used for supplying the feed, medium, acid and base solutions for pH control.

3.3. Reactor instrumentation

To maintain the pH of the system a pH meter and a controller have been provided. pH has been maintained by addition of acid or base from the tanks provided at the top. The oxygen content in the reaction medium was measured using a DO meter. The flow rate of air can be measured using a rotameter, with a range of 0.167×10^{-4} to $1.67 \times 10^{-4} \text{ m}^3/\text{s}$ (1–10 lpm).

3.4. Microbial culture

A strain of microorganism *Pseudomonas* sp. (SP-1) reported to be capable of utilizing phenol as the sole carbon and energy source was obtained from Regional Research Laboratory, Jammu, India.

3.5. Culture preparation

Inoculum was prepared by growing the bacteria on $2.6 \times 10^{-3} \text{ m}^3$ (2.6 l) of 0.05 kg/m^3 (50 ppm) of phenol solution containing growth medium. Before inoculation of the organism sterilization of the phenol solution was done in autoclave at a gage pressure of $1.034 \times 10^5 \text{ N/m}^2$ (15 psi) for 20 min.

3.6. Growth medium

The growth medium was made up using tap water. Sterile conditions were not maintained during the continuous operation of the reactor, to simulate treatment of actual plant wastewater as the latter would contain different contaminants.

3.7. Biomass

25 ml of the sample was withdrawn from the reactor and filtered through $0.7 \mu\text{m}$ filter paper to separate the biomass produced. The filter paper was dried at 105°C and weighed again after drying to obtain the weight of the biomass produced.

3.8. Start-up of the equipment

Initially the fluidized bed bioreactor was operated in batch mode for 36 h for immobilization of microorganism onto the solid particles. Subsequently, operation was changed to continuous mode with a feed flow rate of 510 ml h^{-1} (corresponding to the dilution rate of 0.196 h^{-1}) of inlet phenol concentration of about 64 ppm. The dissolved oxygen (DO) concentration in the reactor was maintained at 2 ppm using air initially and subsequently using pure oxygen. The pH in all the runs was maintained at 7.0 using 0.1N HCl and 0.1N NaOH. The reaction temperature was maintained at 30°C . The concentration of phenol in the overflow from the reactor was analyzed for every 1 h iodometrically [19].

3.9. Determination of kinetic parameters and yield coefficients

Experiments were conducted to measure the biokinetic parameters, viz., maximum specific growth rate (μ_{max}), inhibition constant (K_I) and Monod constant (K_S). Experiments were conducted in batch mode in shake flask with different initial phenol concentrations ranging from 64 to 1254 ppm. Nutrients as shown in Table 1 were added to the flasks and the medium was inoculated. Phenol concentration was measured periodically. For each batch run specific growth rate was calculated from the phenol concentration vs. time data. The kinetic parameters mentioned above were determined from the data of specific growth rate vs. phenol initial concentration obtained above by regression analysis (Fig. 2).

Table 1
Composition of growth medium.

Compound	Concentration, ppm
KH_2PO_4	420
K_2HPO_4	375
$(\text{NH}_4)_2\text{SO}_4$	240
NaCl	15
CaCl_2	15
$\text{MgSO}_4 \cdot \text{H}_2\text{O}$	30

For determination of yield coefficient ($Y_{X/S}$, mass of biomass produced per mass of phenol consumed), 25 ml of the reactor medium was taken in every run and filtered through $0.7 \mu\text{m}$ filter paper to separate the biomass produced. The filter paper was dried and weighed. Phenol concentration was determined and the ratio of the biomass produced to the phenol consumed was determined as the yield coefficient.

3.10. Determination of biofilm density (ρ_v) and biofilm thickness

The biofilm density in terms of mass of dry biomass per volume of biofilm was measured as follows: A sample of biomass-laden particles was withdrawn from the reactor and the volume (V_1) of bioparticles was found using a measuring cylinder. The particles were then transferred to a weighed sample vial and placed in oven at 105°C to remove all the moisture. The amount of moisture was found from the difference in weights before and after drying. Now the beads were washed to remove all the attached biomass and the weight of the biomass was found from the difference in weights before and after washing. Now the volume (V_2) of the clean particles was found. The volume of the biofilm is the difference between V_1 and V_2 . The biofilm density was then calculated from the mass of the biomass and the volume of biofilm. From the volume of the biofilm and the radius of the bare particle, the biofilm thickness has been obtained.

4. Simulation of FBR by FFANN

4.1. Construction of FFANN and evaluation of error function

A simple, multilayer FFANN consisting of one input layer with a single neuron, one hidden layer with five hidden neurons and an output layer with a single neuron has been chosen for the solution of differential equations. Each neuron in the hidden layer uses sigmoid function as its activation function, and each neuron in the output layers uses purelin function as its activation function. Two networks (one for phenol and one for oxygen) are needed with the same architecture to solve the given model equations, because given system has two equations and they have to be solved simultaneously.

The input to both networks is the dimensionless biofilm thickness, x . The outputs from the networks 1 and 2 are the dimen-

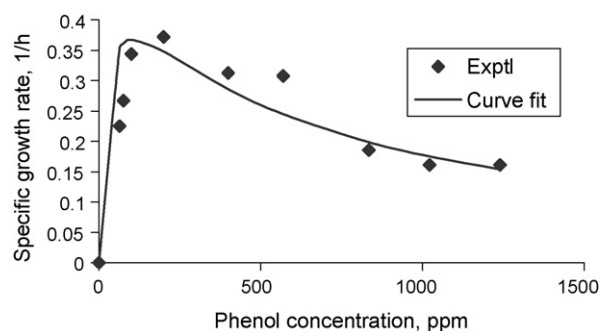


Fig. 2. Specific growth rate as function of substrate concentration.

sionless phenol and oxygen concentrations within the biofilm S^* and C^* , respectively. S^* and C^* can be written as (detailed procedure in Appendix A)

$$S^* = \sum_{i=1}^5 v_{1i} \phi(w_{1i}x + u_{1i}) + u_{1out} \quad (14)$$

$$C^* = \sum_{i=1}^5 v_{2i} \phi(w_{2i}x + u_{2i}) + u_{2out} \quad (15)$$

The dimensionless concentration derivatives can be written as

$$\frac{dS^*}{dx} = \sum_{i=1}^5 v_{1i} w_{1i} \phi'(w_{1i}x + u_{1i}) \quad (16)$$

$$\frac{dC^*}{dx} = \sum_{i=1}^5 v_{2i} w_{2i} \phi'(w_{2i}x + u_{2i}) \quad (17)$$

$$\frac{d^2S^*}{dx^2} = \sum_{i=1}^5 v_{1i} w_{1i}^2 \phi''(w_{1i}x + u_{1i}) \quad (18)$$

$$\frac{d^2C^*}{dx^2} = \sum_{i=1}^5 v_{2i} w_{2i}^2 \phi''(w_{2i}x + u_{2i}) \quad (19)$$

where the subscripts 1 and 2 refer to networks 1 and 2, respectively.

w_{1i} , w_{2i} denote the weight from the input unit to the hidden unit i

v_{1i} , v_{2i} denote the weight from the hidden unit i to the output unit

u_{1i} , u_{2i} denote the bias of hidden unit i

u_{1out} , u_{2out} denote the bias of output unit

ϕ' , ϕ'' denote first and second derivatives of sigmoid transfer function, respectively.

Once the values of S^* and C^* and their derivatives with respect to x is evaluated, the error function can be calculated as shown below.

$$E_1(x) = \left[\left\{ \frac{d^2S^*}{dx^2} + \frac{2}{(x+r_p/\delta)} \frac{dS^*}{dx} - \phi_s \frac{S^*}{(S^*+K_s+S^{*2}/K_i)} \frac{C^*}{(C^*+K_o)} \right\}^2 + \left\{ \frac{d^2C^*}{dx^2} + \frac{2}{(x+r_p/\delta)} \frac{dC^*}{dx} - \phi_o \frac{S^*}{(S^*+K_s+S^{*2}/K_i)} \frac{C^*}{(C^*+K_o)} \right\}^2 \right] \quad (20)$$

$$E_2(x) = \left[\left\{ \frac{dS^*}{dx} \right\}^2 + \left\{ \frac{dC^*}{dx} \right\}^2 \right] \quad \text{if } x \text{ is } 0 \quad (21)$$

$$E_2(x) = \left[\left\{ \frac{dS^*}{dx} - B_{is}(1-S^*) \right\}^2 + \left\{ S^* - S_i^* \right\}^2 + \left\{ \frac{dC^*}{dx} - B_{io}(1-C^*) \right\}^2 \right] \quad \text{if } x \text{ is } 1 \quad (22)$$

The integration domain $x \in [0,1]$ can be discretized in to finite number of points. $x = [0,0.1,0.2, \dots, 1.0]$. Then the mean squared error will be calculated as follows:

$$MSE = \left(\frac{1}{11} \right) \sum_i E_1(x_i) + \left(\frac{1}{2} \right) \sum_j E_2(x_j) \quad (23)$$

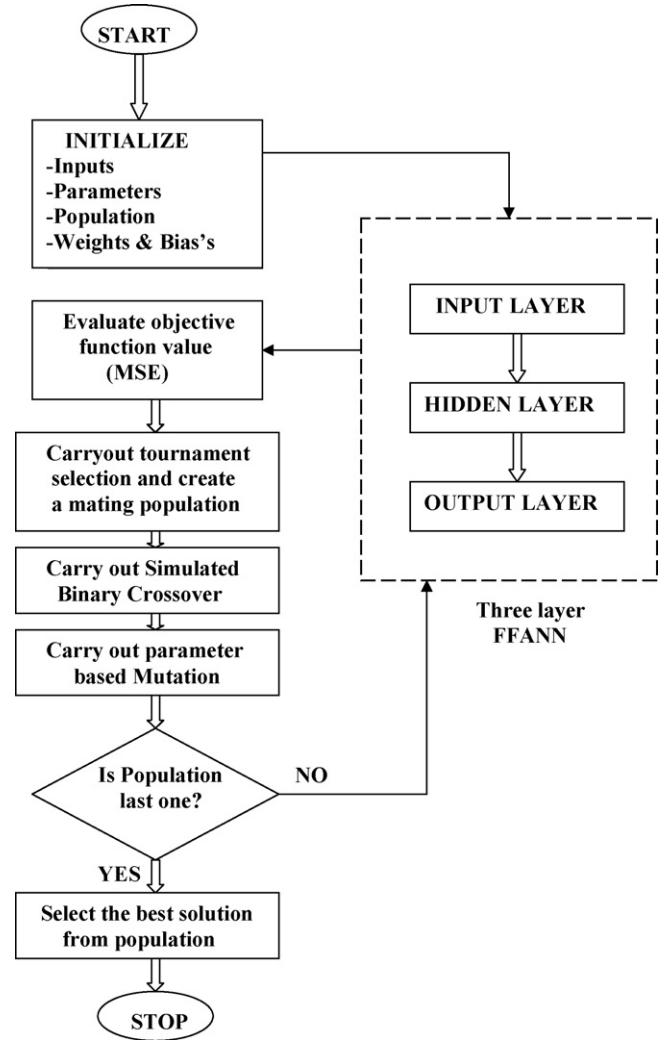


Fig. 3. Flow chart for implementing real-coded GA for FFANN training.

5. Results and discussion

The model equations describing the biodegradation process within the biofilm in an FBR were solved using an FFANN trained with a real-coded GA to find out the diffusivities of substrates in the biofilm. The flow chart of the combinational FFANN and GA has been shown in Fig. 3. The model parameters used for this work are given in Table 2. A MATLAB script was developed to solve a system of ordinary differential equations using FFANN trained with real-coded GA.

Table 2
Model parameters for the estimation of diffusivities in the biofilm.

Parameter	Value	Units
μ_{max}	1.427×10^{-4}	s^{-1}
K_s	21.92×10^{-3}	kg/m^3
K_i	522×10^{-3}	kg/m^3
K_o	0.26×10^{-3}	kg/m^3
$Y_{x/s}$	0.62	kg/kg
$Y_{x/o}$	0.465	kg/kg
k_s	0.4×10^{-4}	m/s
k_o	0.65×10^{-4}	m/s
N_p	6369	–
r_p	2.155×10^{-3}	m/s
δ	19.1×10^{-6}	m
ρ_v	170.6–226.9	kg/m^3

Table 3
Simulation results for different flow rates of feed water.

Flow rate of feed water Q (ml/h)	S_b (ppm)	$R_{obs} \times 10^4$ (kg/h)	S_i (ppm)	C_i (ppm)	$R_{calc} \times 10^4$ (kg/h)	Diffusivities		Biot number Bi_s	Difference between R_{obs} and R_{calc} (%)	MSE $\times 10^4$
						In the biofilm $\times 10^9$ (m^2/s)				
						phenol D_{ef}	oxygen D_{of}			
390	51	4.69	42.38	1.737	4.72	0.035	0.332	21.72	0.72	5.87
510	57	6.08	45.82	1.857	6.03	0.053	0.369	14.53	1.02	1.82
600	59	7.15	45.88	1.901	7.14	0.054	0.382	14.05	0.21	2.90
640	65	7.64	50.98	1.923	7.61	0.055	0.392	13.86	0.32	0.79

S_b, S_i —concentration of phenol in bulk liquid phase and at the liquid biofilm interface, respectively, R_{obs}, R_{calc} —observed and calculated rate of phenol degradation, respectively.

5.1. FFANNs for solving ODEs

Network specifications:

- Type: Feedforward artificial neural network
- Transfer functions: Sigmoid (hidden layer) and pure linear (output layer)
- Error criterion: Mean squared error
- Architecture: One input layer with one neuron, one hidden layer with 5 neurons, and one output layer with one neuron.
- Training method: Unsupervised training using real-coded GA
- Mode of training: Batch mode

The architecture of the network was selected by a trail and error procedure starting with a simple structure of one hidden layer with 3 neurons (the input and output layer has each one neuron which is fixed by the problem). The number of neurons in the hidden layer was increased progressively up to 15. Decrease in error with respect to increase in hidden neurons was observed. The network with five neurons in the hidden layer was found to be sufficient for the present problem. No attempt was made to find out the optimum number of hidden layers, since it would be better to select a network with minimum number of hidden layers so that the number of parameters to be optimized will be less in the training phase. A batch mode of training was adapted, in which the weights are updated after the presentation of all the training examples that constitute an epoch.

5.2. Training FFANN by real-coded genetic algorithms

It has been observed in literature [20,21] that real-coded GAs are the best suited for the minimization of error of a multilayer FFANN, especially when the gradient of the error surface to be minimized is not available at hand, as such the present problem. In the present study the MSE decreased from starting values of more than ten to the order of 10^{-2} in around 2000 generations for all the runs. Further, it took more generations for fine-tuning of error. This is comparatively far less than conventional backpropagation algorithms, which has been reported to take a minimum of 20,000–1,00,000 epochs to converge to a global solution [22]. Though no trials were made to find out optimum parameters for GA, it worked well with a selection pressure of 40% and crossover probability of 0.6 [20].

Real-coding offers the advantage of avoiding encoding and decoding problems associated with binary coding, hence easier implementation. Though the SBX operator has an advantage of not using the upper and lower bound for the weights [23], it was found that the number of generations required for that case was more in comparison with the one with upper and lower bound. Hence, the algorithm with upper and lower bound was used for the present work. The upper and lower bound for the weights were found using a trail and error method and are in the range of -10 to $+10$.

The use of parameter based mutation enhances the fine search because, as the generations increases, the mutation probability also increases linearly with generation number starting from $1/20$ to 1 (starting from one variable in the first generation to all variables in the last generation), the search field is getting shrunk and more number of variables are mutated. This follows the suggestion in literature [20,24,25] of more dependency towards mutation for GA training of ANNs. As expected the implementation was comparatively easier since the gradient of the error surface is not calculated in GA training.

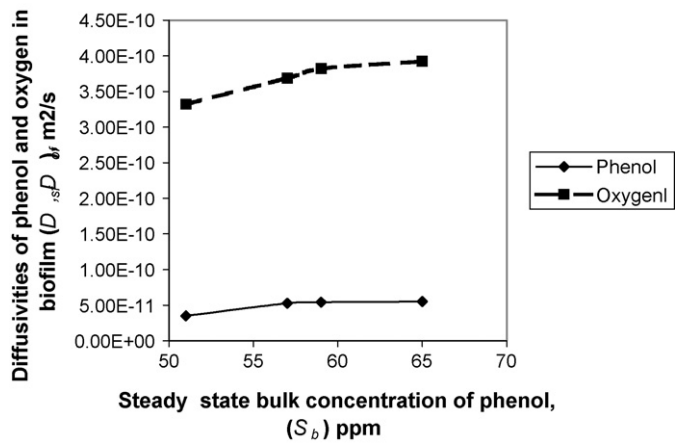


Fig. 4. Diffusivities of phenol and oxygen in biofilm vs. steady state bulk concentration of phenol.

5.3. Estimation of diffusivities in the biofilm of an FBR

By knowing the experimental values of S_b and C_b , the model Eqs. (9)–(13) were solved to find diffusivities of oxygen and phenol in the biofilm relative to their values in water. This has been done by adjusting the relative diffusivities in such a way that both degradation rates (R_{scal} and R_{sobs}) will become equal. In the present work, diffusivities of oxygen and phenol are adjusted until the difference between degradation rates become less than 1%. The simulated diffusivities and their relative values with water are presented in Table 3. The relative diffusivities are varying in the range of 0.041–0.065. The reason for the low values of diffusivities is the high biofilm density. Since in a biofilm with a higher density the number of cells and amount of exopolymer per unit biofilm volume would be higher [3], the resistance to diffusion of phenol and oxygen through the biofilm would be greater. The result of lesser diffusivities therefore appears to be reasonable. Sensitivity analysis shows that a change of 10–15% in the diffusivities has been found to increase the relative error to 4–5%.

It is found from the results that these values are in reasonable agreement with the values reported in the literature. Tang and Fan [3] reported that the relative diffusivities were in the range of 0.086–0.245 for biofilm densities in the range of 151–72 kg/m³. Livingston and Chase [12] reported a relative diffusivity of 0.05 for a biofilm with a density of 217 kg/m³ and with a biofilm thickness of 24.4 μ m (these conditions are closer to the present problem).

Another observation from the results shows that the diffusivities are slightly increasing with flow rate of feed water. This would be

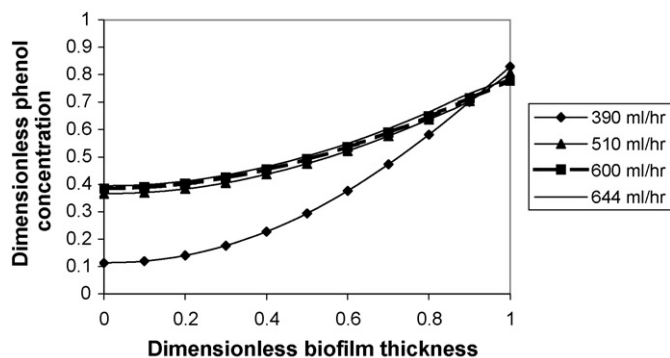


Fig. 5. Dimensionless biofilm thickness vs. dimensionless phenol concentration.

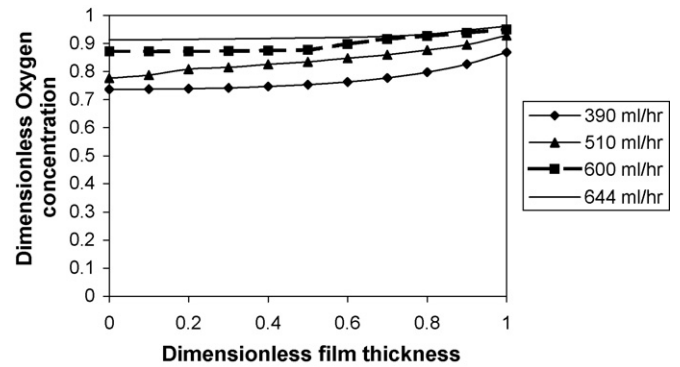


Fig. 6. Dimensionless biofilm thickness vs. dimensionless oxygen concentration.

the result of increase in steady state concentration of phenol (S_b) with flow rate and this is clear from Fig. 4. The Biot number for phenol, B_{is} , is listed in Table 3. It ranges from 13.86 to 21.76. The Biot number for a species gives an indication of the relative importance of diffusion vs. reaction. The lower values of Biot number indicate that the mass transfer resistance is important in limiting the overall rate of reaction.

5.4. Concentration profile for phenol

The concentration profile for phenol and oxygen for various flow rates are obtained and presented in Figs. 5 and 6. It can be seen from these figures that, the concentration profile of phenol is steeper, near the liquid biofilm interface, becoming flatter towards the surface of the particle, leading to a conclusion that, the interface mass transfer resistance from liquid to solid (biofilm) is higher than that of the diffusion resistance offered within the biofilm.

5.5. Concentration profile for oxygen

The concentration profile for oxygen is essentially flat within the biofilm, indicating very little mass transfer resistance to diffusion within the biofilm. There is some slope close to the biofilm surface for the feed flow rate of 390 ml/h. Further, the absolute values of oxygen concentration within the biofilm are greater than the value of K_o . This would explain the independency of the biodegradation rate with respect to DO concentration of 2 ppm in the reactor.

5.6. Effect of flow rate on phenol degradation rate

The rate of phenol degradation for various flow rates can be obtained and are presented in Table 3 and Fig. 7. It can be

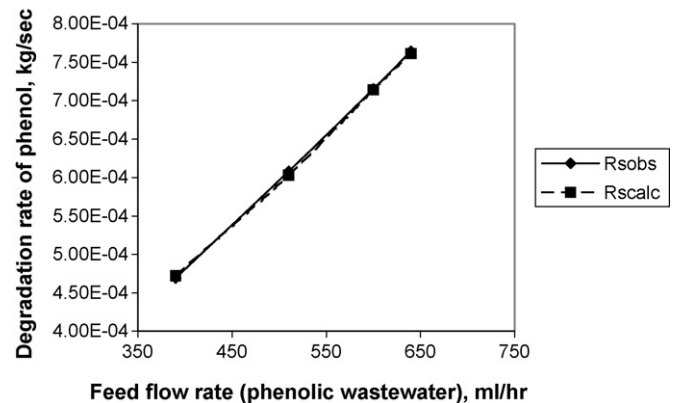


Fig. 7. Degradation rate—observed, Calculated vs. flow rate.

seen from the concentration profiles that, the increase in flow rate decreases the external mass transfer resistance, and hence increases the rate of reaction. From these results it can be concluded that with increase in flow rate the observed as well as calculated rate of phenol degradation are increasing (within the experimental limit).

6. Conclusions

The model equations describing the biodegradation of phenol in a fluidized bed bioreactor have been solved using feedforward artificial neural network and the diffusivities of phenol and oxygen within the biofilm are found. The program script has been developed by using MATLAB. Real-coded genetic algorithm has been used to train the neural network in an unsupervised manner. The networks were trained to a mean squared error level in the range of 10^{-4} . The predicted diffusivities are in reasonable agreement with the literature values. The results show that the diffusivities of phenol and oxygen slightly increase with increase in steady state bulk concentration of phenol, within the experimental range. This result also suggests that the feedforward neural networks trained by real-coded genetic algorithm is a good technique for the simulation of biodegradation process in a fluidized bed bioreactor.

Appendix A. The method

Let us consider a general differential equation in the form:

$$D(f(y)) = 0 \quad (\text{A1})$$

with respect to boundary conditions

$$B(f(y)) = 0 \quad (\text{A2})$$

where D and B are any nonlinear, inhomogeneous differential operators and $f(y)$ is the solution that satisfies Eq. (1) and the boundary conditions (2). Considering that an FFANN is a universal function approximator, the goal of the method is to find a neural network $f^*(y)$ which approximates $f(y)$ in the finite domain $y \in [a, b]^n$.

Consider a multilayer FFANN with n input units, one hidden layer with H sigmoid units and a linear output unit. For a given input vector $\vec{x} = (x_1, \dots, x_n)$ the output of the network N , is given by

$$N = \sum_{i=1}^H v_i \varphi(z_i) + u_{out} \quad (\text{A3})$$

Where

$$z_i = \sum_{j=1}^n w_{ij} x_j + u_i \quad (\text{A4})$$

where w_{ij} denotes the weight from the input unit j to the hidden unit i . v_i denotes the weight from the hidden unit i to the output unit. u_i , u_{out} denote the bias of hidden unit i and output unit, respectively. $\varphi(z_i)$ is the sigmoid transfer function.

Since φ is a continuous and derivable function of x , it can be shown that [6]:

$$\frac{\partial^k N}{\partial x_j^k} = \sum_{i=1}^H v_i w_{ij}^k \varphi^k(z_i) \quad (\text{A5})$$

where φ^k denotes the k th derivative of the sigmoid function.

Hence it is possible to approximate the differential operators D and B using the network; in other words $f(y)$ can be approximated by a network (N) with a differentiable activation function. In order

to find an approximation of $f(y)$, Eq. (1) along with boundary conditions (2) can be chosen as the performance function of the network. The error measure E must be evaluated in a finite number of points (P) into the integration domain $y_i \in [a, b]^n$.

$$E(w) = \frac{1}{P} \sum_i^P [D(f^*(y_i))]^2 + \frac{1}{P_B} \sum_j^{P_B} [B(f^*(y_j))]^2 \quad (\text{A6})$$

P_B is the total number of boundary points and $f^*(y)$ is the approximated output from the network corresponding to the input points (y_i, y_j) . As E tends to zero, f^* tends to f and so the approximate solution for the differential equation system is found. The efficient minimization of Eq. (A6) can be considered as a procedure of training the neural network. At this point, the original problem has been reduced to an unconstrained optimization problem involving the minimization of the error E with respect to the network parameters w_{ij} and u , i.e., weights and biases. Since the error does not depend on target outputs (the function f is unknown a priori) the network is said to be trained in an unsupervised manner.

References

- [1] J.C. Van Den Heuvel, H.H. Beekink, Kinetic effects of simultaneous inhibition by substrate and product, *Biotechnol. Bioeng.* 31 (1988) 718–723.
- [2] W.T. Tang, K. Wisecarver, L.S. Fan, Dynamics of a draft tube gas–liquid–solid FBBR for phenol degradation, *Chem. Eng. Sci.* 42 (1987) 2123–2134.
- [3] W.T. Tang, L.S. Fan, Steady state phenol degradation in a draft-tube fluidized bed bioreactor, *AIChE J.* 33 (1987) 239–249.
- [4] M. Denac, I.J. Dunn, Packed and fluidized bed biofilm reactor performance for anaerobic wastewater treatment, *Biotechnol. Bioeng.* 32 (1986) 159–173.
- [5] D.W. Holladay, C.W. Hancher, D.D. Chilcote, C.D. Scott, Biodegradation of phenolic waste liquors in stirred-tank, columnar and fluidized-bed bioreactors, *Proc. AIChE Symp. Ser.* 74 (1978) 241–252.
- [6] A. Venu Vinod, G. Venkat Reddy, Simulation of biodegradation process of phenolic wastewater at higher concentrations in a fluidized-bed bioreactor, *Biochem. Eng. J.* 24 (2005) 1–10.
- [7] A. Venu Vinod, G. Venkat Reddy, Mass transfer correlation for phenol biodegradation in a fluidized bed bioreactor, *J. Hazard. Mater.* B136 (2006) 727–734.
- [8] C.S.A. Sa, R.A.R. Boaventura, Biodegradation of phenol by *Pseudomonas putida* DSM 548 in a trickling bed reactor, *Biochem. Eng. J.* 9 (2001) 211–219.
- [9] G. Gonzalez, M.G. Herrera, M.T. Garcia, M.M. Pena, Biodegradation of phenol in a continuous process: comparative study of stirred tank and fluidized-bed bioreactors, *Bioresour. Technol.* 76 (2001) 245–251.
- [10] A.G. Livingston, H.A. Chase, Development of a phenol degrading fluidized bed bioreactor for constant biomass hold up, *Chem. Eng. J.* 45 (1991) B35–B47.
- [11] A.M.G. Monteiro Alvaro, R.A.R. Boaventura, A.E. Rodrigues, Phenol biodegradation by *Pseudomonas putida* DSM 548 in a batch reactor, *Biochem. Eng. J.* 6 (2000) 45–49.
- [12] A.G. Livingston, H.A. Chase, Modeling phenol degradation in a fluidized bed bioreactor, *AIChE J.* 35 (1989) 1980–1992.
- [13] L.S. Fan, R. Levya-Ramos, K.D. Wiesecarver, B.J. Zehner, Diffusion of phenol through a biofilm grown on activated carbon particles in a draft-tube three phase fluidized bed bioreactor, *Biotechnol. Bioeng.* 35 (1990) 279–286.
- [14] R.M. Worden, T.L. Donaldson, Dynamics of a biological fixed film for phenol degradation in a FBBR, *Biotechnol. Bioeng.* 30 (1987) 398–412.
- [15] A.J. Meade, A.A. Fernandez, The numerical solution of linear ordinary differential equations by feedforward neural networks, *Math. Comp. Model.* 19 (1994) 1–25.
- [16] A.J. Meade, A.A. Fernandez, Solution of nonlinear ordinary differential equations by feedforward neural networks, *Math. Comp. Model.* 20 (1994) 19–44.
- [17] I.E. Lagaris, A. Likas, D.I. Fotiadis, Artificial neural networks for solving ordinary and partial differential equations, *IEEE Trans. on Neural Networks* 9 (1998) 987–1000.
- [18] D.R. Parisi, M.C. Mariani, M.A. Laborde, Solving differential equations with unsupervised neural networks, *Chem. Eng. Proc.* 42 (2003) 715–721.
- [19] N.H. Furman, *Scott's Standard Methods of Chemical Analysis*, vol. 2, Fifth ed., D. Van Nostrand Co. Inc., New York, 1959.
- [20] J.D. Schaffer, D. Whitley, L.J. Eshelman, Combinations of genetic algorithms and neural networks: a survey of the state of the art, in: L.D. Whitley, J.D. Schaffer (Eds.), *COGANN-92: International Workshop on Combinations of Genetic Algorithms and Neural Networks*, IEEE Computer Society Press, 1992, pp. 1–37.
- [21] Z. Liu, A. Liu, W. Wang, Z. Niu, Evolving neural network using real coded genetic algorithm (GA) for multispectral image classification, *Future Gener. Comp. Syst.* 20 (2004) 1119–1129.
- [22] H. Lee, I. Kang, Neural Algorithms for solving differential equations, *J. Comput. Phys.* 91 (1990) 110–131.

- [23] K. Deb, An efficient constraint handling method for genetic algorithms, *Comput. Methods Appl. Mech. Eng.* 186 (2000) 311–338.
- [24] S. Dominic, D. Whitley, R. Das, C. Anderson, Genetic reinforcement learning for neural networks, in: *IJCNN-91: International Joint Conference on Neural Networks (IEEE Transactions)*, Seattle, 2, 1991, pp. 71–76.
- [25] D.J. Montana, L. Davis, Training feedforward neural networks using genetic algorithms, in: *Proceedings of eleventh international joint conference on artificial intelligence*, Morgan Kaufmann, San Mateo, CA, 1989, pp. 762–767.